Channel Estimation for Millimeter Wave MIMO System: A Sequential Analysis Approach

Jinduo Zhang[1(✉)], Rongfei Fan[2], and Peng Liu[3]

[1] School of Information and Electronics, Beijing Institute of Technology, Beijing, People's Republic of China
3120190835@bit.edu.cn

[2] School of Cyberspace Science and Technology, Beijing Institute of Technology, Beijing, People's Republic of China
fanrongfei@bit.edu.cn

[3] China Ship Research and Development Academy, Beijing, People's Republic of China

Abstract. Channel estimation is crucial for a millimeter wave MIMO system. Due to the existence of massive antenna elements, the overhead to perform channel estimation with traditional methods would be huge, which will degrade the throughput severely. Thanks to the sparsity of channel model on millimeter wave band, most existing literature make use of this feature to compress the number of signaling based on the technique of compressive sensing. In this paper, by making use of the fact that the angle of arrival (AoA) and angle of departure (AoD) vary much slower than the channel coefficients, we go one step forward on saving the number of signaling for channel measurement. Specifically, with a consideration of channel sparsity feature, we design a set of methods to detect the variation of AoA and AoD in time, which includes the case of appearance of new path and disappearance of existing path, through sequential analysis approach. Moreover, to enhance the performance of our proposed method, procoder and combiner are designed respectively to generate beam on anticipated directions, through semi-definite programming method. With the above operations, we only need to measure channel coefficients when the AoA and AoD are not detected to change, which does not require much signaling. Through this way, the overhead for channel measurement is further saved compared with the methods based on compressive sensing.

Keywords: Millimeter wave · Channel measurement · Multiple input multiple output (MIMO) system · Sequential analysis · Semi-definite programming

1 Introduction

Millimeter wave communication technology is one of the most effective technologies for the next generation of wireless communication systems. The short wavelength of millimeter wave can reduce the size of the antenna element and make the use of large-scale antenna arrays feasible [1], which can further increase the gain of the array to combat the deep fading on millimeter wave band. Therefore, a millimeter wave system

W. Hussain and M. A. Jan (Eds.): IoTaaS 2021, LNICST 421, pp. 39–53, 2022.
https://doi.org/10.1007/978-3-030-95987-6_3

generally comes up with the implementation of a massive MIMO system, which is called as millimeter wave MIMO system for the ease of presentation in the following.

For a communication system, in order to achieve high throughput, it is a prerequisite to obtain channel state information (CSI) before sending the information. Millimeter wave MIMO system is not an exception. To acquire the CSI, channel measurement is required, whose task to recover the angle of arrival (AoA) and angle of departure (AoD) and channel coefficient of every path through multiple signaling signals. Recalling traditional channel measurement methods. They mainly include the one based on channel gain's covariance matrix (CCM method) [2] and the one based on spatial basis expansion model (SBEM method) [3], both of which rely on the knowledge of channel gain's covariance matrix. However, due to the huge number of antenna elements in a millimeter wave MIMO system, a lot of signaling will be required to estimate the channel gain's covariance matrix, which is time-consuming. To reduce the signaling overhead, the sparsity of channel model for millimeter wave signal prorogation is made use of and the channel measurement methods are developed based on compressing sensing (CS) theory in literature [4–6]. On the other hand, one more feature of the millimeter wave channel model is omitted in current related research works: The coherence time of every path's AoA and AoD is much larger than the coherence time of the path's channel coefficient [7]. With such a feature, it is possible to only estimate every path's channel coefficient when the associated AoA and AoD do not change, which will surely saving signaling overhead compared with the channel measurement methods based CS theory. As a complement, one more method is required to detect the change of channel's AoA or AoD.

In this paper, we realize the above idea for the channel measurement of millimeter wave MIMO system with the aid of sequential analysis approach. Specifically, we categorize the change of channel's AoA or AoD into two cases: 1) The appearance of new path; 2) The disappearance of existing path. For each case, in order to save signaling overhead, a quickest detection problem is formulated, which targets at minimizing the delay for detecting the variation of investigated statistics, and the Cumulative Sum (CUSUM) method is proposed to serve as the solution. To enhance the performance of detection (to make the divergence between the investigated statistics before change and after change to be larger), the precoder at the transmitter and the combiner at the receiver are proposed to be designed. In response to every case of AoA/AoD variation, two types of beamforming problems are formulated, which are shown to be non-convex. With some transformations and relaxation, we change the formulated beamforming problems into two semi-definite programming (SDP) problems, which are convex. Optimal solution and a good-enough feasible solution for the original two beamforming problems can be found based on the solutions obtained by solving the transformed SDP problems, respectively.

2 System Model

Consider a millimeter wave MIMO system with one transmitter and one receiver. There are N_T antennas at the transmitter and N_R antennas at the receiver, both of which are aligned in unitary linear array (ULA). To overcome the hardware limitation, a hybrid analog and digital beamforming architecture is adopted at both the transmitter and the receiver. The hybrid analog and digital beamforming architecture is the concatenation of a low-dimensional digital beamformer and a high-dimensional analog beamformer. For the hybrid beamforming structure at the transmitter, the overall precoder $\mathbf{v} \in \mathbb{C}^{N_T \times 1}$ can be written as $\mathbf{v} = \mathbf{V}^{RF} \times \mathbf{v}^D$, where $\mathbf{V}^{RF} \in \mathbb{C}^{N_T \times N_t^{RF}}$ is the RF precoding matrix and $\mathbf{v}^D \in \mathbb{C}^{N_t^{RF} \times 1}$ is the digital precoding matrix. For the receiver, the overall precoder $\mathbf{w} \in \mathbb{C}^{N_R \times 1}$ can be written as $\mathbf{w} = \mathbf{W}^{RF} \times \mathbf{w}^D$, where $\mathbf{W}^{RF} \in \mathbb{C}^{N_R \times N_r^{RF}}$ is the RF precoding matrix and $\mathbf{w}^D \in \mathbb{C}^{N_r^{RF} \times 1}$ is the digital precoding matrix. For an analog precoder, only phase can be shifted, thus there are $|\mathbf{V}^{RF}(i,j)| = 1$ and $|\mathbf{W}^{RF}(i,j)| = 1$, where $\mathbf{V}^{RF}(i,j)$ and $\mathbf{W}^{RF}(i,j)$ indicate the element of matrix $\mathbf{W}^{RF}$ and $\mathbf{V}^{RF}$ on ith row and jth column, respectively. We assume the $N_t^{RF} \geq 2N_T$ and $N_r^{RF} \geq 2N_R$. In this case, the hybrid structure is equivalent with the full digital beamformer[8].

With such a hybrid structure, suppose the transmitted signal $s = 1$ without loss of generality, then the broadcasted signal at the N_T antennas of the transmitter, denoted as $\mathbf{x}$, can be written as

$$\mathbf{x} = \mathbf{v}s = \mathbf{V}^{RF}\mathbf{v}^D s = \mathbf{V}^{RF}\mathbf{v}^D \tag{1}$$

Suppose $\mathbf{H} \in \mathbb{C}^{N_R \times N_T}$ is the channel matrix and $\mathbf{z} \sim \mathcal{CN}(\mathbf{0}, \sigma^2 \mathbf{I}_{N_R})$, then the received signal at N_R antennas of the receiver, denoted as $\mathbf{y}_0 \in \mathbb{C}^{N_R \times 1}$, can be written as

$$\mathbf{y}_0 = \mathbf{H}\mathbf{x} + \mathbf{z}, \tag{2}$$

and the received signal, denoted as y, can be written as

$$\begin{aligned} y &= \mathbf{w}^H \mathbf{H}\mathbf{x} + \mathbf{w}^H \mathbf{z} \\ &= \mathbf{w}^H \mathbf{H}\mathbf{v} + \mathbf{w}^H \mathbf{z} \end{aligned} \tag{3}$$

For the channel matrix $\mathbf{H}$, suppose there are N_S scatters, denote $\mathcal{N}_S \triangleq \{1, 2, ..., N_S\}$, $\mathbf{H}$ can be written as

$$\mathbf{H} = \sum_{n=1}^{N_S} \alpha_n \boldsymbol{\alpha}_r(\phi_n^\dagger) \boldsymbol{\alpha}_t^H(\theta_n^\dagger) \tag{4}$$

where α_n is the channel coefficient, $\phi_n^\dagger$ is the AoD, and the $\theta_n^\dagger$ is the AoA, of nth path for $n \in \mathcal{N}_S$. Specifically,

$$\boldsymbol{\alpha}_t(\theta_n^\dagger) = \frac{1}{\sqrt{N_T}} \left[1, e^{j\frac{2\pi}{\lambda} d \sin(\theta_n^\dagger)}, ..., e^{j\frac{2\pi}{\lambda} d \sin(\theta_n^\dagger)(N_T - 1)}\right]^T \tag{5}$$

and

$$\boldsymbol{\alpha}_r(\phi_n^\dagger) = \frac{1}{\sqrt{N_R}} \left[1, e^{j\frac{2\pi}{\lambda} d \sin(\phi_n^\dagger)}, ..., e^{j\frac{2\pi}{\lambda} d \sin(\phi_n^\dagger)(N_R - 1)}\right]^T \tag{6}$$

where d is the inter-antenna spacing and λ is the wavelength of signal. According to [9], N_S is no larger than 4. Moreover, the α_n changes more frequently than $\phi_n^\dagger$ and $\theta_n^\dagger$ for $n \in \mathcal{N}_S$ [7].

Before channel estimation, we do not know the set of $\{\theta_n\}$ and $\{\phi_n\}$. Thus we need to represent the channel matrix $\mathbf{H}$ in another way. Discretize all the AoD as N_D

uniformly-spaced angles, which are denoted as θ_1, ..., θ_{N_D}, and all the AoA as N_A uniformly-spaced angles, which are denoted as ϕ_1, ..., ϕ_{N_A}. Note that both $N_D \gg N_S$ and $N_A \gg N_S$. Denote

$$\boldsymbol{\Gamma}_t = \left[\boldsymbol{\alpha}_t\left(\theta_1\right), \boldsymbol{\alpha}_t\left(\theta_2\right), ..., \boldsymbol{\alpha}_t\left(\theta_{N_D}\right)\right], \tag{7}$$

$$\boldsymbol{\Gamma}_r = \left[\boldsymbol{\alpha}_r\left(\phi_1\right), \boldsymbol{\alpha}_r\left(\phi_2\right), ..., \boldsymbol{\alpha}_r\left(\phi_{N_A}\right)\right], \tag{8}$$

where $\boldsymbol{\Gamma}_t \in \mathbb{C}^{N_T \times N_D}$ and $\boldsymbol{\Gamma}_r \in \mathbb{C}^{N_R \times N_A}$. Then we can write $\mathbf{H}$ as

$$\mathbf{H} = \boldsymbol{\Gamma}_r \boldsymbol{\Lambda} \boldsymbol{\Gamma}_t^H \tag{9}$$

where $\boldsymbol{\Lambda} \in \mathbb{C}^{N_A \times N_D}$ is a sparse matrix only with N_S non-zero elements. When $\theta_i = \theta_n^*$ and $\phi_j = \phi_n^*$ for $n \in \mathcal{N}_S$, the element of $\boldsymbol{\Lambda}$ on ith column and jth row is α_n for $n \in \mathcal{N}_S$. All the other elements of $\boldsymbol{\Lambda}$ are zero. For the ease of discussion in the following, we vectorize $\mathbf{H}$ as $\text{vec}(\mathbf{H}) \in \mathbb{C}^{N_T N_R \times 1}$, define $\boldsymbol{\Psi} \triangleq \boldsymbol{\Gamma}_t^* \otimes \boldsymbol{\Gamma}_r$ where $\otimes$ is the Kronecker product, and $\mathbf{h} \triangleq \text{vec}(\boldsymbol{\Lambda}) \in \mathbb{C}^{N_D N_A \times 1}$ which is a sparse vector with N_S non-zero elements, then (9) can be rewritten as

$$\text{vec}(\mathbf{H}) = \boldsymbol{\Psi}\mathbf{h}. \tag{10}$$

and (3) can be rewritten as

$$\begin{aligned} y &= (\mathbf{v}^T \otimes \mathbf{w}^H)\text{vec}(\mathbf{H}) + \mathbf{w}^H\mathbf{z} \\ &= (\mathbf{v}^T \otimes \mathbf{w}^H)\boldsymbol{\Psi}\mathbf{h} + \mathbf{w}^H\mathbf{z} \end{aligned} \tag{11}$$

Suppose at time instant k, the associated precoding vector is $\mathbf{v}_k$ and the combining vector is $\mathbf{w}_k$, the received signal is y_k, then there is

$$y_k = (\mathbf{v}_k^T \otimes \mathbf{w}_k^H)\boldsymbol{\Psi}\mathbf{h} + \mathbf{w}_k^H\mathbf{z} \tag{12}$$

Hence the channel measurement is to reconstruct $\boldsymbol{h}$ from a number of y_k for $k = 1, 2, ...$

3 Brief Procedure

With the above system model, we focus on two special features of the investigated millimeter wave MIMO system:

- The maximal number of scatters N_S, denoted as $N_S^{\max}$, is no larger than 4.
- The α_n changes more frequently than $\phi_n^\dagger$ and $\theta_n^\dagger$ for $n \in \mathcal{N}_S$.

These two features motives us to reconstruct $\mathbf{h}$ with less number of measurements compared with the methods based on CS, which is given as follows

- Design an algorithm to closely monitor the change of $\phi_n^\dagger$ and $\theta_n^\dagger$ for $n \in \mathcal{N}_S$.
- When $\phi_n^\dagger$ and $\theta_n^\dagger$ for $n \in \mathcal{N}_S$ change and is detected by our designed monitoring algorithm, traditional channel estimation method, such as the CS method, can be resorted to so as to estimate the newly changed $\phi_n^\dagger$ and $\theta_n^\dagger$ for $n \in \mathcal{N}_S$, and the associated α_n for $n \in \mathcal{N}_S$.

– When $\phi_n^\dagger$ and $\theta_n^\dagger$ for $n \in \mathcal{N}_S$ is detected to be unchanged, current $\phi_n^\dagger$ and $\theta_n^\dagger$ for $n \in \mathcal{N}_S$ is effective. Hence we know which element of $\mathbf{h}$ is non-zero. Additionally, since the number of scatters N_S is no larger than 4, only 4 elements of $\mathbf{h}$ is needed to be estimated. In this case, 4 samples of y_k is enough to reconstruct $\mathbf{h}$, i.e., α_n for $n \in \mathcal{N}_S$, according to [10][1].

Through this way, it can be easily found that the number of y_k can be saved since $\phi_n^\dagger$ and $\theta_n^\dagger$ for $n \in \mathcal{N}_S$ does not need to be estimated compared with the channel measurement methods based on CS theory, which estimates not only α_n but also $\phi_n^\dagger$ and $\theta_n^\dagger$ for $n \in \mathcal{N}_S$ in every instance. This type of reduction of y_k samples would be significant since α_n changes more frequently than $\phi_n^\dagger$ and $\theta_n^\dagger$ for $n \in \mathcal{N}_S$.

In the following, we focus on designing the algorithm that can realize our idea. Specifically, we design the precoder and combiner, which can enhance the performance of monitoring whether there is a change of AoA or AoD. In terms of AoA/AoD change detection, we transform it into a quickest detection problem in the area of sequential analysis and propose the CUSUM method to serve as a solution. When the angle disappearance is being detected, we amplify the monitored path and suppress other scattering paths. Detailed discussion will be expanded in the following two sections.

4 Design of Precoder and Combiner

On the change of $\phi_n^\dagger$ and $\theta_n^\dagger$ for $n \in \mathcal{N}_S$, one of the following two cases may happen:

– Case I: Disappearance of one or more existing path.
– Case II: Appearance of one or more path, which does exist currently.

In the following two subsections, how to design precoder and combiner for Case I and Case II will be discussed, respectively.

4.1 Design of Precoder and Combiner for Case I

For the ease of discussion, the following notations are made. Since one path can be composed of one combination of ϕ_n and θ_n, denote the set of all the possible paths as $\mathcal{P} \triangleq \{1, 2, ..., N_A N_D\}$ and the set of currently existing paths as $\mathcal{P}_S$, where $\mathcal{P}_S \subset \mathcal{P}$ and $|\mathcal{P}_S| = |\mathcal{N}_S| = N_S$. For $p \in \mathcal{P}$, the associated path gain, AoA, and AoD are written as $\alpha_{n(p)}$, $\phi_{n(p)}$, and $\theta_{n(p)}$, respectively. Without loss of generality, we investigate the received signal at time instant k, y_k. Then by referring to (3) and (4), y_k can be written as

$$y_k = \sum_{p \in \mathcal{P}_S} \alpha_{n(p)} \mathbf{w}_k^H \boldsymbol{\alpha}_r(\phi_{n(p)}) \cdot \boldsymbol{\alpha}_t^H(\theta_{n(p)}) \mathbf{v}_k + \mathbf{w}_k^H \mathbf{z} \tag{13}$$

When one of the existing paths, denoted as path p^*, is being observed for disappearance, the signal from the paths $\mathcal{P}_S \setminus \{p^*\}$ should be isolated, thus there should be

$$v_k^H \boldsymbol{\alpha}_t(\theta_{n(p)}) = 0, \forall p \in \mathcal{P}_S \setminus \{p^*\} \tag{14}$$

[1] If the number of samples y_k is more than 4, the estimation accuracy of α_n for $n \in \mathcal{N}_S$ would be higher, which depends on the selection of user in real application.

at the precoder, and

$$w_k^H \boldsymbol{\alpha}_r(\phi_{n(p)}) = 0, \forall p \in \mathcal{P}_S \setminus \{p^*\} \tag{15}$$

at the combiner. The constraints (14) and (15) can be written as the following equivalent form, respectively.

$$\mathbf{v}_k^H \boldsymbol{\Lambda}_t(\theta_{n(p)})\mathbf{v}_k = 0, \forall p \in \mathcal{P}_S \setminus \{p^*\} \tag{16}$$

$$\mathbf{w}_k^H \boldsymbol{\Lambda}_r(\phi_{n(p)})\mathbf{w}_k = 0, \forall p \in \mathcal{P}_S \setminus \{p^*\} \tag{17}$$

where $\boldsymbol{\Lambda}_t(\theta_{n(p)}) \triangleq \boldsymbol{\alpha}_t(\theta_{n(p)})\boldsymbol{\alpha}_t^H(\theta_{n(p)})$ and $\boldsymbol{\Lambda}_r(\phi_{n(p)}) \triangleq \boldsymbol{\alpha}_r(\phi_{n(p)})\boldsymbol{\alpha}_r^H(\phi_{n(p)})$.

In addition, in case that there is new path $p \in \mathcal{P} \setminus \mathcal{P}_S$ appears, the signals coming from the paths in $\mathcal{P} \setminus \mathcal{P}_S$ should also be suppressed, i.e., there should be

$$\mathbf{v}_k^H \left(\sum_{p \in \mathcal{P} \setminus \mathcal{P}_S} \boldsymbol{\Lambda}_t(\theta_{n(p)}) \right) \mathbf{v}_k \leq \varepsilon_t \tag{18}$$

at the precoder and

$$\mathbf{w}_k^H \left(\sum_{p \in \mathcal{P} \setminus \mathcal{P}_S} \boldsymbol{\Lambda}_r(\phi_{n(p)}) \right) \mathbf{w}_k \leq \varepsilon_r \tag{19}$$

at the receiver, where ε_t and ε_r are pre-defined thresholds. At the precoder, there is a maximal transmit power constraint, which can be written as

$$\mathbf{v}_k^H \mathbf{v}_k \leq P_T \tag{20}$$

where P_T is maximal transmit power at the transmitter.

For the precoder, collecting the listed constraints (16), (18), and (20), the problem of designing $\mathbf{v}_k$ can be written as

Problem 1

$$\begin{aligned} \max_{\boldsymbol{v}_k} \quad & \boldsymbol{v}_k^H \boldsymbol{\Lambda}_t(\theta_{n(p^*)})\boldsymbol{v}_k \\ \text{s.t.} \quad & \boldsymbol{v}_k^H \boldsymbol{\Lambda}_t(\theta_{n(p)})\boldsymbol{v}_k = 0, \forall p \in \mathcal{P}_S \setminus \{p^*\}, & \text{(21a)} \\ & \boldsymbol{v}_k^H \left(\sum_{p \in \mathcal{P} \setminus \mathcal{P}_S} \boldsymbol{\Lambda}_t(\theta_{n(p)}) \right) \boldsymbol{v}_k \leq \varepsilon_t, & \text{(21b)} \\ & \boldsymbol{v}_k^H \boldsymbol{v}_k \leq P_T. & \text{(21c)} \end{aligned}$$

For the design of combiner, the problem of designing $\mathbf{w}_k$ can be given as

Problem 2

$$\begin{aligned} \min_{\boldsymbol{w}_k} \quad & \boldsymbol{w}_k^H \boldsymbol{w}_k \\ \text{s.t.} \quad & \boldsymbol{w}_k^H \boldsymbol{\Lambda}_r(\phi_{n(p^*)})\boldsymbol{w}_k \geq \tau_r, & \text{(22a)} \\ & \boldsymbol{w}_k^H \boldsymbol{\Lambda}_r(\phi_{n(p)})\boldsymbol{w}_k = 0, \forall p \in \mathcal{P}_S \setminus \{p^*\}, & \text{(22b)} \\ & \boldsymbol{w}_k^H \left(\sum_{p \in \mathcal{P} \setminus \mathcal{P}_S} \boldsymbol{\Lambda}_r(\phi_{n(p)}) \right) \boldsymbol{w}_k \leq \varepsilon_r, & \text{(22c)} \end{aligned}$$

where τ_r is the pre-define threshold for guaranteeing the received signal strength from path p^*.

Both Problem 1 and Problem 2 are non-convex. A broadly used method to solve such kind of optimization problem via SDP method [11]. Specifically, define $\boldsymbol{A} \bullet \boldsymbol{B} \triangleq \text{tr}\,(\boldsymbol{A}\boldsymbol{B})$. Then $\mathbf{x}^H \mathbf{A}\mathbf{x} = \mathbf{A} \bullet \mathbf{x}\mathbf{x}^H$. Define $\mathbf{W}_k = \mathbf{w}_k^H \mathbf{w}_k$ and $\mathbf{V}_k = \mathbf{v}_k^H \mathbf{v}_k$, Problem 1 and Problem 2 can be relaxed to be

Problem 3

$$
\begin{aligned}
\max_{\boldsymbol{V}_k} \quad & \boldsymbol{V}_k \bullet \boldsymbol{\Lambda}_t(\theta_{n(p^*)}) \\
\text{s.t. } & \boldsymbol{V}_k \bullet \boldsymbol{\Lambda}_t(\theta_{n(p)}) = 0, \forall p \in \mathcal{P}_S \setminus \{p^*\}, && \text{(23a)} \\
& \boldsymbol{V}_k \bullet \left(\sum_{p \in \mathcal{P} \setminus \mathcal{P}_S} \boldsymbol{\Lambda}_t(\theta_{n(p)}) \right) \le \varepsilon_t, && \text{(23b)} \\
& \boldsymbol{V}_k \bullet \boldsymbol{I} \le P_T, && \text{(23c)} \\
& \boldsymbol{V}_k \succeq 0, && \text{(23d)}
\end{aligned}
$$

and

Problem 4

$$
\begin{aligned}
\min_{\boldsymbol{W}_k} \quad & \boldsymbol{W}_k \bullet \boldsymbol{I} \\
\text{s.t.} \quad & \boldsymbol{W}_k \bullet \boldsymbol{\Lambda}_r(\phi_{n(p^*)}) \ge \tau_r, && \text{(24a)} \\
& \boldsymbol{W}_k \bullet \boldsymbol{\Lambda}_r(\phi_{n(p)}) = 0, \forall p \in \mathcal{P}_S \setminus \{p^*\}, && \text{(24b)} \\
& \boldsymbol{W}_k \bullet \left(\sum_{p \in \mathcal{P} \setminus \mathcal{P}_S} \boldsymbol{\Lambda}_r(\phi_{n(p)}) \right) \le \varepsilon_r, && \text{(24c)}
\end{aligned}
$$

respectively.

It can be noticed that by adding the constraint $\text{rank}\,(\mathbf{V}_k) = 1$ and $\text{rank}\,(\mathbf{W}_k) = 1$ into Problem 3 and Problem 4, they would turn to be equivalent with Problem 1 and Problem 2, respectively. Thus if the optimal solution of Problem 3 or Problem 4 is rank-one, it is also the optimal solution of Problem 1 or Problem 2.

According to Corollary 4.6 of [12], there is rank-one optimal solution for Problem 3 and Problem 4, which can be found by following Algorithm 2 of [12]. Hence by following Algorithm 2 of [12], we can find the optimal solution of Problem 1 and Problem 2, respectively.

4.2 Design of Precoder and Combiner for Case II

For Case II, we do not know which path will appear. To detect the appearance of some path, we need to scan over all the possible AoDs ($\{\theta_n | n = 1, 2, ..., N_A\}$) while keeping the combiner to be omnidirectional, and scan over all the possible AoAs ($\{\phi_n | n = 1, 2, ..., N_D\}$) while keeping the precoder to be omnidirectional, respectively. In the following, we will show how to generate beamforming vectors for scanning over all the possible AoDs while keeping the combiner to be omnidirectional. How to generate beamforming vectors to scan all the possible AoAs can be realized in a similar way and is omitted for brevity.

To speed up the scanning process, we divide N_D angles of AoD into multiple clusters, each one of which has equal number of AoD angles. Then we can scan AoD angles cluster by cluster. At the precoder, suppose the ith cluster is being investigated, i.e., the set of AoD angles being investigated is $\mathcal{N}_{D_i} \subset \mathcal{N}_D \triangleq \{1, 2, ..., N_D\}$. Note that $\mathcal{N}_{D_i} \cap \mathcal{N}_{D_j} = \emptyset$, $\bigcup\limits_i \mathcal{N}_{D_i} = \mathcal{N}_D$, and $|\mathcal{N}_{D_i}| = |\mathcal{N}_{D_j}|$. Then the problem of designing $\mathbf{v}_k$ can be written as

Problem 5

$$\begin{aligned} \max_{\boldsymbol{v}_k, t_T} \quad & t_T \\ \text{s.t.} \quad & \boldsymbol{v}_k^H \boldsymbol{\Lambda}_t(\theta_n) \boldsymbol{v}_k \geq t_T, \forall n \in \mathcal{N}_{D_i}, && \text{(25a)} \\ & \boldsymbol{v}_k^H \left(\sum_{n \in \mathcal{N}_D \setminus \mathcal{N}_{D_i}} \boldsymbol{\Lambda}_t(\theta_n) \right) \boldsymbol{v}_k \leq \varepsilon_{ts}, && \text{(25b)} \\ & \boldsymbol{v}_k^H \boldsymbol{v}_k \leq P_T, && \text{(25c)} \end{aligned}$$

where ε_{ts} is the pre-defined threshold.

For the combiner, the omnidirectional beamforming problem of designing $\mathbf{w}_k$ can be given as

Problem 6

$$\begin{aligned} \max_{\boldsymbol{w}_k, t_R} \quad & t_R \\ \text{s.t.} \quad & \boldsymbol{w}_k^H \boldsymbol{\Lambda}_r(\phi_n) \boldsymbol{w}_k \geq t_R, \forall n \in \mathcal{N}_A, && \text{(26a)} \\ & \boldsymbol{w}_k^H \boldsymbol{w}_k \leq \varepsilon_{rs}, && \text{(26b)} \end{aligned}$$

where ε_{rs} is the pre-defined value for the purpose of suppressing the noise power of received signal.

By following the SDP relaxation method in Sect. 4.1, Problem 5 and Problem 6 can be relaxed to be

Problem 7

$$\begin{aligned} \max_{\boldsymbol{V}_k, t_T} \quad & t_T \\ \text{s.t.} \quad & \boldsymbol{V}_k \bullet \boldsymbol{\Lambda}_t(\theta_n) \geq t_T, \forall n \in \mathcal{N}_{D_i}, && \text{(27a)} \\ & \boldsymbol{V}_k \bullet \left(\sum_{n \in \mathcal{N}_D \setminus \mathcal{N}_{D_i}} \boldsymbol{\Lambda}_t(\theta_n) \right) \leq \varepsilon_{ts}, && \text{(27b)} \\ & \boldsymbol{V}_k \bullet \boldsymbol{I} \leq P_T, && \text{(27c)} \\ & \boldsymbol{V}_k \succeq 0, && \text{(27d)} \end{aligned}$$

and

Problem 8

$$\max_{\boldsymbol{W}_k, t_R} \quad t_R$$
$$\text{s.t. } \boldsymbol{W}_k \bullet \boldsymbol{\Lambda}_r(\phi_n) \geq t_R, \forall n \in \mathcal{N}_A, \tag{28a}$$
$$\boldsymbol{W}_k \bullet \boldsymbol{I} \leq \varepsilon_{rs}, \tag{28b}$$
$$\boldsymbol{W}_k \succeq 0, \tag{28c}$$

respectively.

Problem 7 and Problem 8 can be solved by bisection searching the maximal t_T or t_R such that the constraints in (27) and (28) are feasible respectively, which involves SDP for every given t_T or t_R.

Since the vector $\boldsymbol{\alpha}_t(\theta_{n(p)})$ and $\boldsymbol{\alpha}_r(\theta_{n(p)})$ for $p \in \mathcal{P}$ are Vandermonde, then according to [13], there is rank-one optimal solution for Problem 7 and Problem 8. Unfortunately, how to generate the rank-one optimal solution for the type of problem like Problem 7 and Problem 8 is not characterized in [13]. Here we resort to Gaussian sampling method to generate the rank-one solution [14].

5 AoA/AoD Change Detection

5.1 Problem Formulation for Case I: Disappearance of Path

In this case, with the precoder and combiner implemented as the way in Sect. 4.1, we get a sequence of received signal $y_k, k = 1, 2, ...$ for watching the p^*th path. There is a time Γ_{I}, before which the path p^* is still active and after which the path p^* disappears. Before Γ_{I}, the sequence of $y_k, k = 1, 2, ...$ are subject to one distribution, denoted as $f_0^{\text{I}}(x)$, independently. For $f_0^{\text{I}}(x)$, since $\mathbf{z} \sim \mathcal{CN}(\mathbf{0}, \sigma^2 \mathbf{I}_{N_R})$ and combining the fact in (13), $f_0^{\text{I}}(x)$ is a Gaussian distribution conditioned on $\alpha_{n(p^*)}$, which can be also denoted as $f_0^{\text{I}}(x|\alpha_{n(p^*)})$, with mean being $\left(\alpha_{n(p^*)} \mathbf{w}_k^H \boldsymbol{\alpha}_r(\phi_{n(p^*)}) \cdot \boldsymbol{\alpha}_t^H(\theta_{n(p^*)}) \mathbf{v}_k\right)$ and variance being $\sigma^2 \mathbf{w}_k^H \mathbf{w}_k$. As previously assumed, $\alpha_{n(p^*)}$ is a complex Gaussian random variable with mean being zero and variance being P_{att}. After time Γ_{I}, the sequence of $y_k, k = 1, 2, ...$ are subject to distribution $f_1^{\text{I}}(x)$ independently, which is a Gaussian distribution with mean being 0 and variance being $\sigma^2 \mathbf{w}_k^H \mathbf{w}_k$.

Define $\mathbb{P}_t$ and $\mathbb{E}_t$ as the probability measure and corresponding expectation under the event $\{\Gamma^{\text{I}} = t\}$. Hence $\mathbb{P}_\infty$ and $\mathbb{E}_\infty$ denote the case $t = \infty$. Our target is to find a stopping time T^{I}, such that the disappearance of the path p^* is declared once it happens. By following the problem formulation of Lorden's quickest change detection, define

$$d_t(T^{\text{I}}) = \operatorname{ess\,sup} \mathbb{E}_t \left[\left(T^{\text{I}} - t + 1\right)^+ | \mathcal{F}_{t-1} \right] \tag{29}$$

and

$$d(T^{\text{I}}) = \sup_{t \geq 1} d_t(T^{\text{I}}), \tag{30}$$

where $(x)^+ = \max(x, 0)$ and $\mathcal{F}_t = \sigma(y_1, y_2, ..., y_t)$. The function $d(T^{\text{I}})$ is actually a measure of detection delay. Our target is to solve the following optimization problem

Problem 9

$$\min_{T^{\mathrm{I}}\in\mathcal{T}} \quad d(T^{\mathrm{I}})$$
$$s.t.\ \mathbb{E}_{\infty}[T^{\mathrm{I}}] \geq \eta \tag{31a}$$

where $\mathcal{T} \triangleq \{T|\mathbb{E}_t[T] < \infty\}$. This is a change-point detection problem in the field of sequential analysis.

5.2 Problem Formulation for Case II: Appearance of Path

In this case, the AoA or AoD of a new appearing path will be disjoint from the ones in existing paths. Thus we need to detect the appearance of a new AoA or AoD angle separately so as to catch the appearance of a new path. With the precoder and combiner implemented as the way in Sect. 4.2 and suppose the cluster being watched is i, we get a sequence of received signal y_k^i, $k = 1, 2, ...$ To study the case in a more convenient way, we turn to investigate the signal $|y_k^i|$, $k = 1, 2, ...$ The sequence of $\{|y_k^i|\}$ falls into one of the falling two hypothesis

$$\mathcal{H}_0 : |y_k^i| \overset{i.i.d.}{\sim} f_0^{\mathrm{II}}(x), k = 1, 2, ...$$
$$\mathcal{H}_1 : |y_k^i| \overset{i.i.d.}{\sim} f_1^{\mathrm{II}}(x), k = 1, 2, ...$$

For ith sector under hypothesis $\mathcal{H}_0$, $f_0^{\mathrm{II}}(x)$ may be uncertain.

- When there is no path appearing in all the other sectors, $f_0^{\mathrm{II}}(x)$ would be a Rice distribution with ν_0 being 0 and σ_0 being $\sqrt{\sigma^2 \mathbf{w}_k^H \mathbf{w}_k}$, where ν_0 and σ_0 are parameters in the PDF of Rice distribution. The PDF of Rice distribution can be written as

$$f(x|\nu_0, \sigma_0) = \frac{x}{\sigma_0^2} e^{\frac{-(x^2+\nu_0^2)}{2\sigma_0^2}} I_0\left(\frac{x\nu_0}{\sigma_0^2}\right)$$

  where $I_0(y)$ is the first kind modified Bessel function with order zero.
- When there are $(N_S^{\max} - N_S)$ paths appearing in every other sector rather than ith sector, $f_0^{\mathrm{II}}(x)$ would be a Rice distribution with ν_0 being $|\alpha_n|\left(N_S^{\max} - N_S\right)\sqrt{\varepsilon_{ts} t_R^{\max}}$ at most and σ_0 being $\sqrt{\sigma^2 \mathbf{w}_k^H \mathbf{w}_k}$. Note that α_n represents the random channel coefficient, which is complex Gaussian random variable with mean being 0 and variance being P_{att}, and

$$t_R^{\max} \triangleq \max_{n\in\mathcal{N}_A} |\boldsymbol{w}_k^H \boldsymbol{\alpha}_r(\phi_n)|.$$

For ith sector under hypothesis $\mathcal{H}_1$, $f_1^{\mathrm{II}}(x)$ may be uncertain either.

- When there is only one path appearing in ith sector and there is no path appearing in all the other sectors, $f_1^{\mathrm{II}}(x)$ would be a Rice distribution with ν_0 being $|\alpha_n|\sqrt{t_T t_R}$ and σ_0 being $\sqrt{\sigma^2 \mathbf{w}_k^H \mathbf{w}_k}$.

– Where there are $(N_S^{\max} - N_S)$ paths in ith sector, $f_1^{\mathrm{II}}(x)$ would be a Rice distribution with ν_0 being $|\alpha_n| \left(N_S^{\max} - N_S\right) \sqrt{t_T^{\max} t_R^{\max}}$ where

$$t_T^{\max} \triangleq \max_{n \in \mathcal{N}_D} |\mathbf{v}_k^H \boldsymbol{\alpha}_t(\theta_n)|,$$

and σ_0 being $\sqrt{\sigma^2 \mathbf{w}_k^H \mathbf{w}_k}$.

Denote the index of cluster we are observing at time k is s_k. Then the observed sequence can be written as $\{y_k^{s_k}; k = 1, 2, ...\}$, which generates a filtration $\{\mathcal{G}_k, k = 1, 2, ...\}$ where $\mathcal{G}_k = \sigma(y_1^{s_1}, y_2^{s_2}, ..., y_k^{s_k})$. Define $\varpi_k(\mathcal{G}_k)$ as the $\mathcal{G}_k$-measurable switching function at time k. $\varpi_k(\mathcal{G}_k) = 0$ indicates that we decide to continue to watch on s_kth sequence, i.e., $s_{k+1} = s_k$; $\varpi_k(\mathcal{G}_k) = 1$ means that we switch to observe the next sequence, i.e., $s_{k+1} = s_k + 1$. Denote Υ as the set of stopping time associated with the filtration $\mathcal{G}_k$ [15]. There should be also one stopping time $\tau \in \Upsilon$ indicating that when we should stop sampling and claim the current observed sequence is subject to $\mathcal{H}_1$, i.e., sequence s_k is subject to $\mathcal{H}_1$ when $\tau = k$.

Our purpose is to optimize the stopping time τ and the switching rule $\varpi = \{\varpi_1, \varpi_2, ...\}$ to minimize the a mixed measure of false alarm probability and average sampling number, $\Pr(\mathcal{H}^{s_\tau} = \mathcal{H}_0) + c\mathbb{E}[\tau]$, where c is positive constant. Suppose the stopping time is no larger than T^{II}, i.e., we have to stop by time T^{II}. The T^{II} can be the maximal number of samples in one fading block or a fraction of it for the purpose of suppressing the overhead of channel sensing. Summarizing all the constraints and the objective function, the specific optimization problem can be formulated as follows

Problem 10

$$\begin{aligned} &\inf_{\tau, \varpi} \Pr(\mathcal{H}^{s_\tau} = \mathcal{H}_0) + c\mathbb{E}[\tau] \\ &s.t. \;\; 0 \le \tau \le T^{II}, \\ &\qquad \tau \in \Upsilon. \end{aligned} \tag{32}$$

5.3 Solution for Case I and Case II

To detect the disappearance and appearance of a path, according to [16], the CUSUM algorithm can serve as a solution, which is usually asymptotic optimal for change point detection problems like the form of Problem 9 or Problem 10. In essence, it can detect the change point of distribution for the observed random time series with low delay. Assume the investigated sequential signal is o_k, $k = 1, 2, ...$, with a change point of distribution at n. The sequences o_k before and after n are supposed to be independent and identically distributed. The distribution before n is f_0(x), and the distribution after n is f_1(x). Then the statistic of CUSUM method can be given as $Z_k = \max\left\{0, Z_{k-1} + \log \frac{f_1(o_k)}{f_0(o_k)}\right\}$ for $k \ge 1$ and $Z_k = 0$ for $k = 0$.

Set a threshold h, if $Z_t \ge h$, we can claim that the distribution of the observed sequence has changed. The threshold h can be selected to satisfy the required constraint of formulated optimization problem through Mont Carlo simulation.

6 Numerical Results

In this section, numerical results are presented to verify the effectiveness of our proposed method. The major system parameters are set as follows. $N_T = 128$ and $N_R = 128$. $N_D = N_A = 20$. The total transmit power $P_T = 1$. $N_S = 4$. The AoA and AoD of every path are randomly generated between $[0, 2\pi]$. The wavelength is $\lambda = 0.001$ m, and the distance between adjacent antenna elements is $\frac{\lambda}{2}$. In terms of SDP problem, CVX toolbox is utilized with default setting. All the ε (including ε_t, ε_r, ε_{ts}, and ε_{rs}) when solving a SDP problem is 0.001.

First, in order to prove the effectiveness of the CUSUM algorithm, we compared it with the traditional binary detection algorithm. We are investigating a sequential sequence with 1000 samples, the change-point of which happens at 501. We set different thresholds for the CUSUM algorithm and the traditional binary detection algorithm, and obtained the detection delay and false alarm probability of the two algorithms under these thresholds, and compared the performance of the two algorithms. In Fig. 1 and Fig. 2, the time delay and false alarm probability under various selection of h is plotted. These two figures can help to characterize the relationship between detection time delay and false alarm probability.

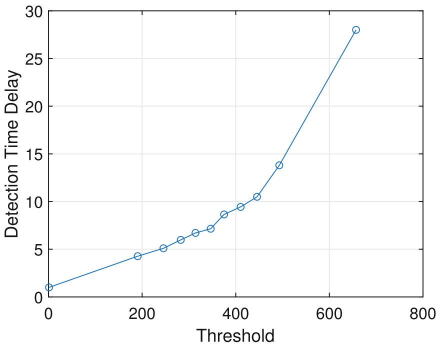

Fig. 1. Time delay of CUSUM

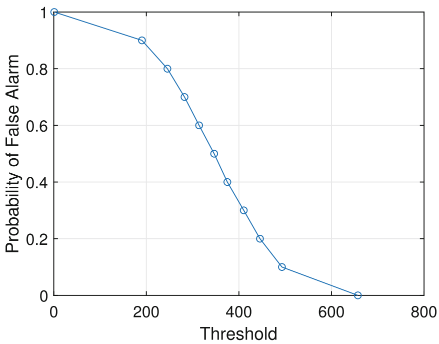

Fig. 2. False alarm of CUSUM

In Fig. 3, the performance of CUSUM is compared with the performance of traditional binary detection method, which is respective of the detection delay. It can be seen from Fig. 3 that the CUSUM method can always outperform the binary detection method, which proves the effectiveness of the CUSUM method.

And most importantly, we compared our algorithm with the traditional OMP algorithm. We assume that the channel coefficient changes 10 times in a fading block of the angles, so for the traditional algorithm, in an angle fading block, we use 10 times of OMP algorithm for channel estimation. On the other hand, for our algorithm, we use the CUSUM algorithm in the detection process and the least squares estimation algorithm in estimating the channel coefficients.

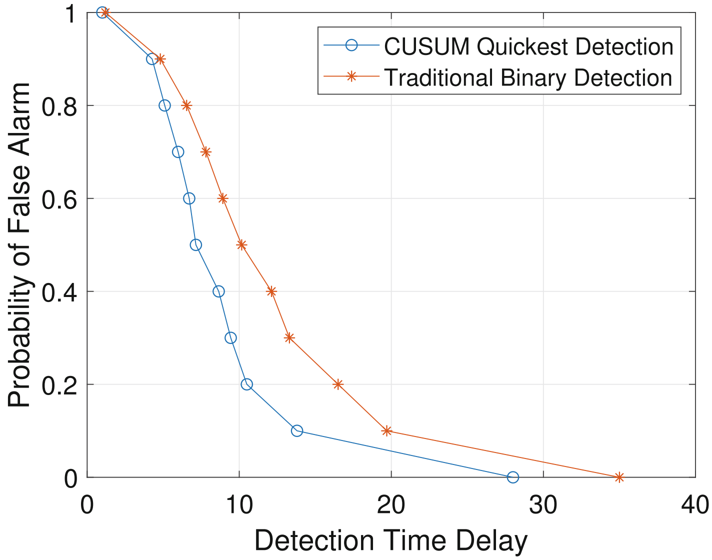

Fig. 3. Comparison of CUSUM and binary detection

In our algorithm, we first detect whether the angle disappears, and then detect whether the angle appears, if a change is detected, we use the OMP algorithm to re-estimate the channel, otherwise we only estimate the channel coefficient. In the process of detecting the disappearance of the angle, we check each current path in turn. On the other hand, in the process of detecting angle generation, we inspect all sectors in turn. In addition, we discretize the angle into 20 parts, and when detecting whether the angle is generated, divide the angle into 5 sectors, where each sector contains 4 discrete angles. The longest number of observation points in a detection is 20, which means that if the number of observation points exceeds 20 and no change is detected, then we determine that the channel angle remains unchanged We compare the relationship between the number of observation points of the two algorithms and the NMSE under three different SNR (3.2 dB, 0 dB, −2.6 dB).

It can be seen from Fig. 4 that under different Signal-to-Noise Ratios(SNR), when the same observation points are used, the NMSE of the current algorithm is smaller than that of the OMP algorithm, which means that when the same NMSE is reached, the number of observation points used by our algorithm is less than that of the traditional OMP algorithm.

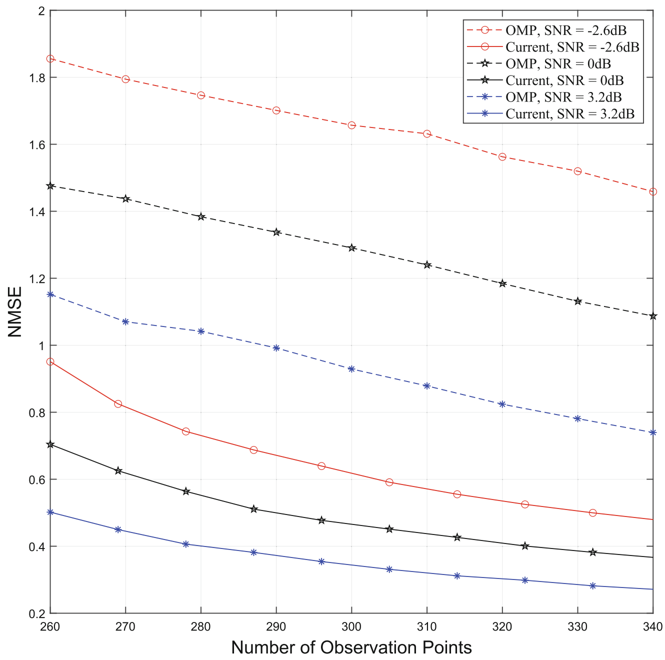

Fig. 4. Comparison of current method and OMP method

7 Conclusion

In this paper, we propose a method of channel measurement for millimeter MIMO system based on the fact that the AoA/AoD coherence time is much longer than the one of channel coefficient. To realize our idea, we utilize the CUSUM method to detect the variation of AoA/AoD with low delay, which falls into the area of sequential analysis. To enhance the performance of CUSUM, we design beamforming for both the precoder and combiner. Through SDP, optimal or sub-optimal solution can be achieved for the formulated beamforming problems. The simulation results show that when the same effect is achieved, our algorithm reduces the time overhead compared with the traditional OMP algorithm. Our proposed method can help to save the signaling overhead for the channel measurement.

References

1. Hu, C., Wang, X., Dai, L., Ma, J.: Partially coherent compressive phase retrieval for millimeter-wave massive MIMO channel estimation. IEEE Trans. Sig. Process. **68**, 1673–1687 (2020)
2. Yin, H., Gesbert, D., Filippou, M., Liu, Y.: A coordinated approach to channel estimation in large-scale multiple-antenna systems. IEEE J. Sel. Areas Commun. **31**(2), 264–273 (2013)
3. Xie, H., Gao, F., Zhang, S., Jin, S.: A unified transmission strategy for TDD/FDD massive MIMO systems with spatial basis expansion model. IEEE Trans. Veh. Technol. **66**(4), 3170–3184 (2017)

4. Xie, H., González-Prelcic, N.: Dictionary learning for channel estimation in hybrid frequency-selective mmWave MIMO systems. IEEE Trans. Wirel. Commun. **19**(11), 7407–7422 (2020)
5. Heath, R.W., González-Prelcic, N., Rangan, S., Roh, W., Sayeed, A.M.: An overview of signal processing techniques for millimeter wave MIMO systems. IEEE J. Sel. Top. Sig. Process. **10**(3), 436–453 (2016)
6. Alkhateeb, A., Ayach, O.E., Leus, G., Heath, R.W.: Channel estimation and hybrid precoding for millimeter wave cellular systems. IEEE J. Sel. Top. Sig. Process. **8**(5), 831–846 (2014)
7. Va, V., Choi, J., Heath, R.W.: The impact of beamwidth on temporal channel variation in vehicular channels and its implications. IEEE Trans. Veh. Technol. **66**(6), 5014–5029 (2017)
8. Sohrabi, F., Yu, W.: Hybrid digital and analog beamforming design for large-scale antenna arrays. IEEE J. Sel. Top. Sig. Process. **10**(3), 501–513 (2016)
9. Akdeniz, M.R., et al.: Millimeter wave channel modeling and cellular capacity evaluation. IEEE J. Sel. Areas Commun. **32**(6), 1164–1179 (2014)
10. Cheng, P., et al.: Channel estimation for OFDM systems over doubly selective channels: a distributed compressive sensing based approach. IEEE Trans. Commun. **61**(10), 4173–4185 (2013)
11. Boyd, S.P., Vandenberghe, L.: Convex Optimization. Cambridge University Press, Cambridge (2004)
12. Huang, Y., Palomar, D.P.: Rank-constrained separable semidefinite programming with applications to optimal beamforming. IEEE Trans. Sig. Process. **58**(2), 664–678 (2010)
13. Karipidis, E., Sidiropoulos, N.D., Luo, Z.Q: Far-field multicast beamforming for uniform linear antenna arrays. IEEE Trans. Sig. Process. **55**(10), 4916–4927 (2007)
14. Palomar, D.P., Eldar, Y.C.: Convex Optimization in Signal Processing and Communications. Cambridge University Press, Cambridge (2010)
15. Zou, S., Veeravalli, V.V., Li, J., Towsley, D.: Quickest detection of dynamic events in networks. IEEE Trans. Inf. Theory **66**(4), 2280–2295 (2020)
16. Tartakovsky, A., Nikiforov, I., Basseville, M.: Sequential Analysis: Hypothesis Testing and Changepoint Detection. CRC Press, Florida (2014)